Strangeness production with ALICE at the LHC

Maria Vasileiou On behalf of the ALICE Collaboration

Physics Department, National and Kapodistrian University of Athens, Athens, Greece

E-mail: mvasili@phys.uoa.gr

Abstract

The main goal of the ALICE experiment is to study the physics of strongly interacting matter under extremely high temperature and energy density conditions to investigate the properties of the Quark-Gluon plasma (QGP). The enhanced production of strange hadrons with respect to non-strange particles was historically considered as one of the signatures of QGP formation during the evolution of the system created in heavy-ion collisions. The excellent tracking and particle identification capabilities of the ALICE experiment allow the reconstruction of multi-strange baryons via their weak decay channels over a large range of transverse momentum. The yields and the relative production rates of strange and multi-strange particles normalized to pions measured in pp, p–Pb, Pb–Pb and Xe–Xe collisions are presented as a function of particle multiplicity. The strangeness production dependence on the collision energy is also shown. Results are compared to QCD-inspired and statistical hadronization model predictions.

Keywords: ALICE, QGP, strangeness

(Some figures may appear in colour only in the online journal)

1. Introduction

The deconfined state of quarks and gluons, the Quark-Gluon Plasma (QGP), predicted by Quantum Chromodynamics (QCD), can be studied in ultra-relativistic heavy-ion collisions. In these collisions the resulting temperature and energy density are expected to be high enough to produce QGP. Similar conditions are believed to have existed a fraction of the second after the Big Bang before quarks and gluons bound together to form hadrons and heavier particles. ALICE (A Large Ion Collider Experiment) is focusing on the physics of strongly interacting matter at extreme energy densities. The existence of the QGP and its properties are key issues in QCD for understanding color confinement. Recreating this primordial form of matter and understanding how it evolves is expected to shed light on questions about how matter is organized, the mechanism that confines quarks and gluons and the nature of strong interactions. Strangeness production plays role in the study of the hot and dense medium created in heavy ion collisions. As predicted by Rafelski and Muller [1], the enhancement of the relative to pp collisions strangeness production could be one of the signatures of phase transition from the state of hadronic matter to QGP. The ALICE detector is suited for the study of QGP, thanks to its exceptional particle identification capabilities. The latest results on the production of strange and multi-strange hadrons in pp, p–Pb, Pb–Pb and Xe–Xe collisions at the LHC (Large Hadron Collider) are presented. The first observation of strangeness enhancement in high-multiplicity pp collisions relative to low-multiplicity ones, within the pp range of multiplicities, is presented. The measurements are in agreement with the p–Pb collision results, showing that the phenomenon is related to the final state multiplicity created in the collision.

2. Experimental setup

ALICE [2] is a general purpose detector for heavy-ion studies at the CERN LHC. It has unique particle identification capabilities among the LHC experiments, allowing for measurements of particles in a wide range in transverse momentum (p_T). The ALICE detector consists of a central barrel, a forward dimuon spectrometer and other forward detectors dedicated to triggering and centrality selection. The central barrel, located inside a solenoidal magnet (B = 0.5 T), covers the midrapidity region $|\eta| < 0.9$ over the full azimuthal angle. It includes a six-layer
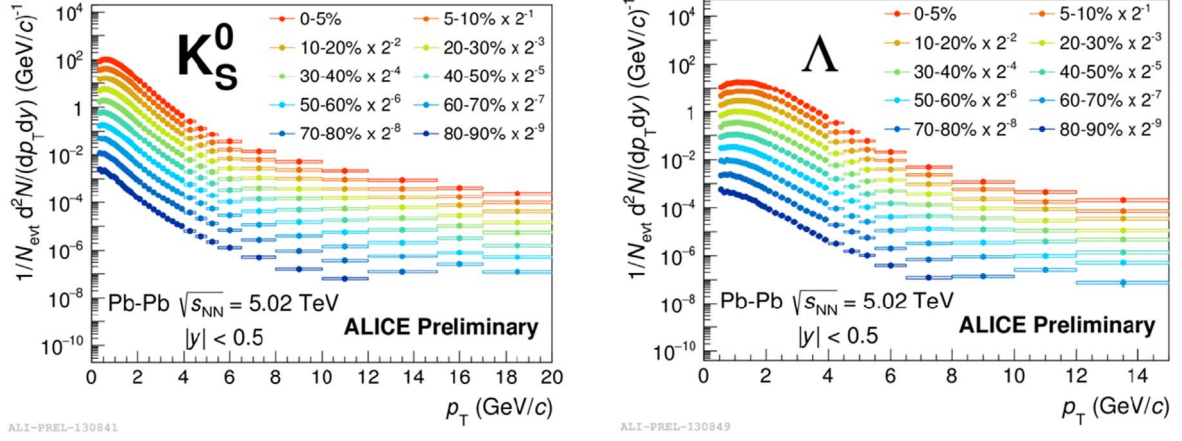
Figure 1. Transverse momentum spectra of K_S^0 and Λ for different centrality classes, as measured in Pb–Pb collisions at $\sqrt{s_{NN}} = 5.02$ TeV. Statistical and systematic uncertainties are plotted as vertical error bars and boxes, respectively.
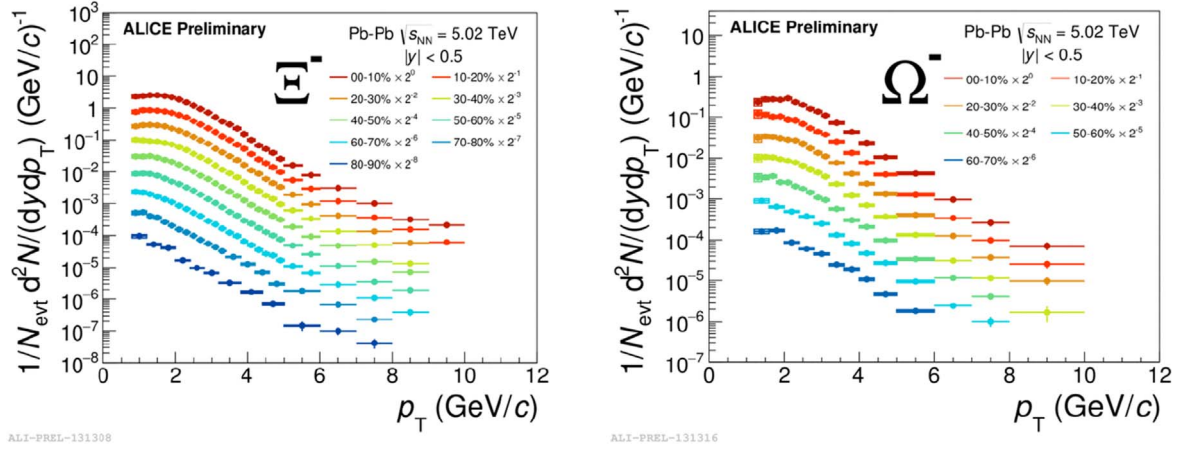
Figure 2. Transverse momentum spectra of Ξ^- and Ω^- for different centrality classes, as measured in Pb–Pb collisions at $\sqrt{s_{NN}} = 5.02$ TeV. Statistical and systematic uncertainties are plotted as vertical error bars and boxes, respectively.

high resolution Inner Tracking System (ITS), a large volume Time Projection Chamber (TPC), electron and charged hadron identification detectors which exploit Transition Radiation (TRD) and Time-Of-Flight (TOF) techniques, respectively. Small area detectors for high-p_T particle identification (HMPID), photon and neutral meson measurement (PHOS), photon and electron ID and jet reconstruction (EMCAL) complement the central barrel. The forward rapidity system includes a single-arm muon spectrometer covering the pseudorapidity rang $-4.0 \leqslant \eta \leqslant -2.5$. Trigge and event multiplicity information is obtained by V0 scintillators, V0A and V0C, which are placed on both sides of the ALICE interaction point. The V0 detector provides minimum bias triggers for central barrel detectors and is used to determine the centrality in heavy-ion collisions. It covers pseudorapidity ranges $2.8 < \eta < 5.1$ (V0A) and $-3.7 < \eta < -1.7$ (V0C).

3. Results and discussion

In the following, results on strangeness production in different collision systems and energies are presented. The single-strange (K_S^0 and Λ) and multi-strange (Ξ and Ω) particles are reconstructed from an invariant mass analysis of their identified hadronic decay product candidates.

3.1. Pb–Pb collisions

The transverse momentum spectra of K_S^0 and Λ in Pb–Pb collisions at $\sqrt{s_{NN}} = 5.02$ TeV are shown in figure 1 for different centrality classes. A hardening of the spectra is observed with increasing centrality. The effect is mass dependent, being more pronounced for heavier particles, and is characteristic of a radial flow. Figure 2 shows the p_T spectra of Ξ^- and Ω^- for different centrality classes in Pb–Pb collisions at $\sqrt{s_{NN}} = 5.02$ TeV. The same pattern, as the one already mentioned for K_S^0 and Λ spectra, is observed for multi-strange hadrons as well. The p_T dependence of the Λ/K_S^0 ratio is presented in figure 3 (left) for two centrality intervals in Pb–Pb collisions at $\sqrt{s_{NN}} = 2.76$ TeV together with model predictions. Figure 2 (right) shows the same ratio as a function of p_T in Pb–Pb collisions at $\sqrt{s_{NN}} = 5.02$ TeV for different centrality intervals. Similar features are observed in Pb–Pb collisions at both energies. There is a depletion at
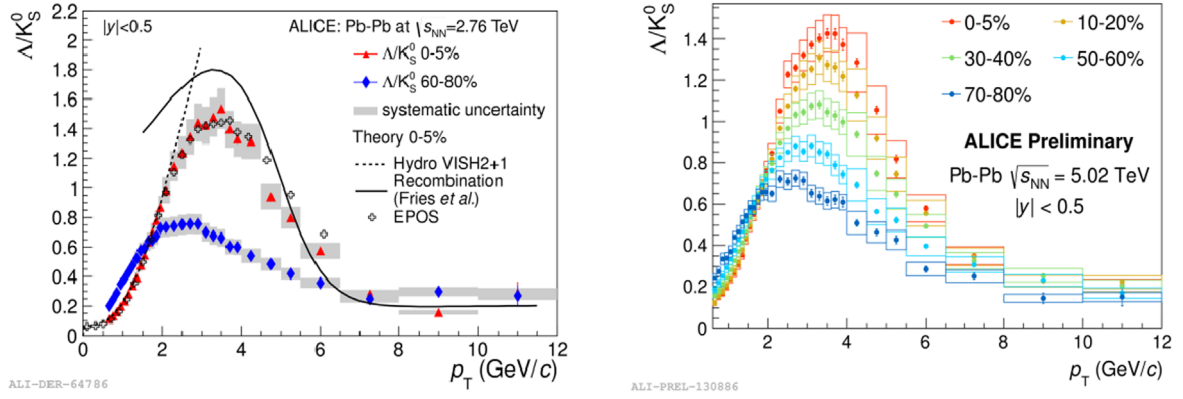
Figure 3. Λ/K_S^0 ratio as a function of p_T for two centrality intervals in Pb–Pb collisions at $\sqrt{s_{NN}} = 2.76$ TeV compared to model predictions (left) and for different centrality intervals in Pb–Pb collisions at $\sqrt{s_{NN}} = 5.02$ TeV (right).
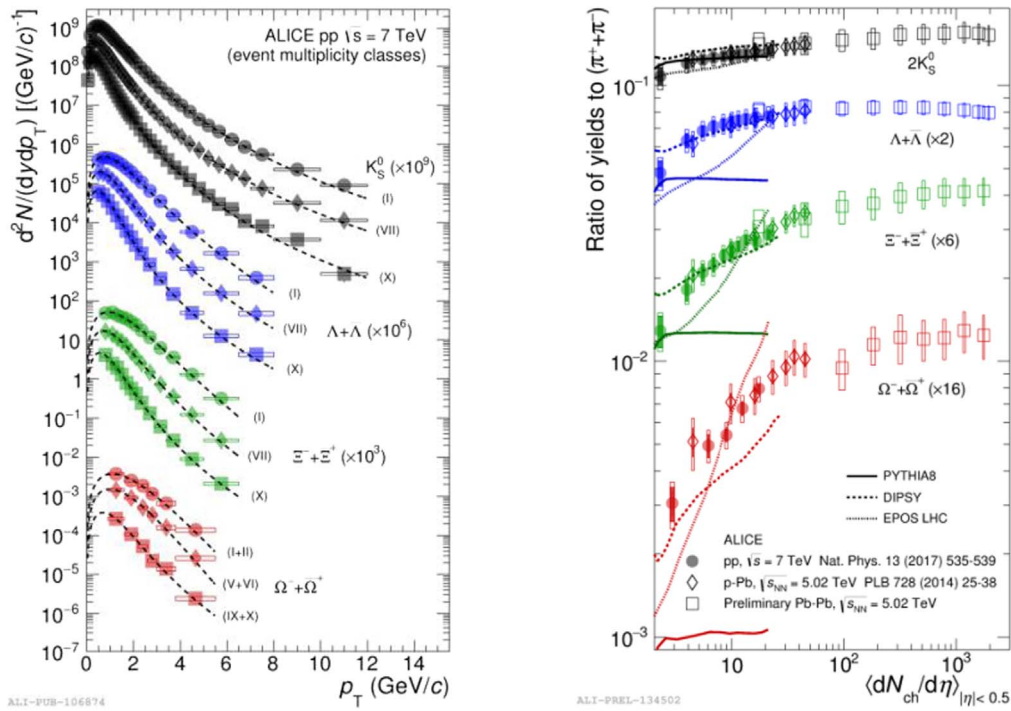

Figure 4. p_T-differential yields of K_S^0, Λ, Ξ and Ω for a selection of multiplicity classes [6]. The data are scaled by different factors to improve visibility. The dashed curves represent Lévy-Tsallis fits (left). p_T-integrated yield ratios of K_S^0, Λ, Ξ and Ω to pions as a function of multiplicity in different collision systems and energies compared to model predictions (right).

low p_T and an enhancement at intermediate p_T. A hydrodynamical model calculation [3] describes the Λ/K_S^0 up to 2 GeV/c rather well but for higher p_T it deviates from the data. Recombination model [4] approximately reproduces the shape but overestimates the baryon enhancement by about 15%. The EPOS Monte Carlo generator [5] describes the ratio over the entire p_T range.

3.2. pp collisions

The p_T distributions of K_S^0, Λ, Ξ and Ω are presented in figure 4 (left) for different multiplicity classes in pp collisions at $\sqrt{s} = 7$ TeV [6]. The evolution of the spectral shapes is similar to the one in Pb-Pb collisions. We observe a hardening of p_T spectra with increasing multiplicity, which is more

pronounced for higher mass particles. In Pb-Pb collisions such behavior is explained by hydrodynamical models. For each particle and each multiplicity class, the p_T- integrated yields are computed by integrating the data over the p_T range of the measurement and by using the integral of a fitted Lévy-Tsallis function in the unmeasured region. The ratio of the yields of K_S^0, Λ, Ξ and Ω to the pion yield is presented if figure 4 (right) as a function of the mean charged-particle multiplicity density, in pp collisions at $\sqrt{s} = 7$ TeV, p–Pb collisions at $\sqrt{s_{NN}} = 5.02$ TeV and Pb–Pb collisions at $\sqrt{s_{NN}} = 5.02$ TeV together with model predictions [7–9]. There is an enhancement of strange to non-strange hadron production going from pp to the most central Pb–Pb collisions. An enhancement is also observed in high- multiplicity pp collisions with respect to low-multiplicity ones. An almost
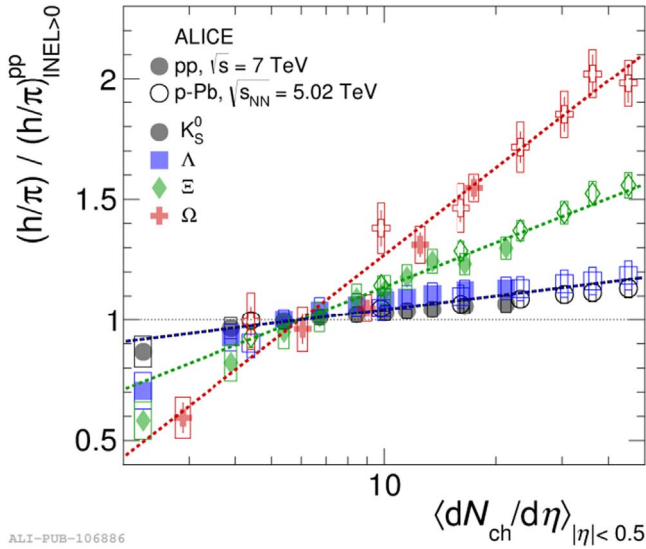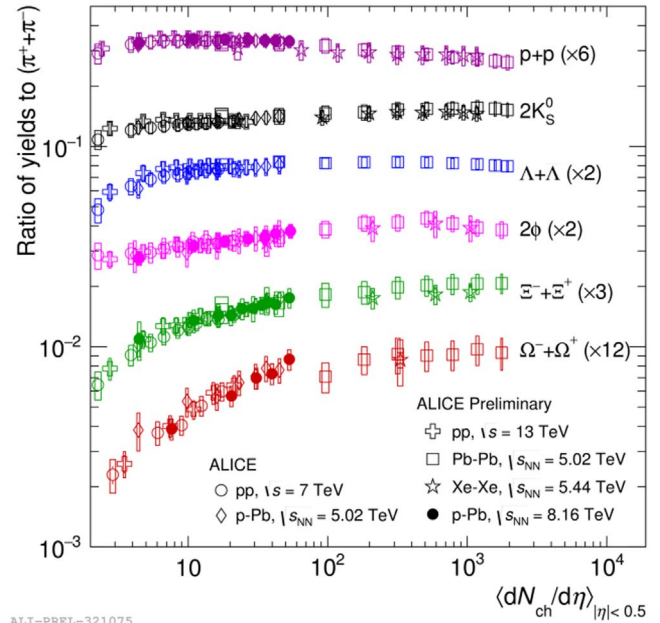
Figure 5. Particle yield ratios to pions normalized to the values measured in the inclusive INEL > 0 pp event class as a function of multiplicity.

Figure 6. Particle yield ratios to pions as a function of multiplicity for different collision systems and energies.

saturated trend is observed in central Pb–Pb collisions for all particle ratios. Since there is no significant dependence on the center-of-mass energy, the origin of strangeness enhancement in hadronic collisions seems to be driven by the final state rather than by the collision system or energy. We observe that none of the models describes the production of strange particles across multiplicity satisfactorily. Figure 5 shows the multiplicity dependence of the K_S^0, Λ, Ξ and Ω yield ratios to pions divided by the values measured in pp events with at least one charged particle in the interval $|\eta| < 1$ (INEL > 0) in pp collisions at $\sqrt{s} = 7$ TeV and p–Pb collisions at $\sqrt{s_{NN}} = 5.02$ TeV [6]. The observed multiplicity dependent enhancement follows a hierarchy determined by the strangeness content of the hadron.

3.3. p–Pb and Xe–Xe collisions

ALICE has measured strangeness in p–Pb collisions at $\sqrt{s_{NN}} = 8.16$ TeV from the 2016 LHC run and preliminary results confirm that no significant collision energy dependence is observed. To compare the relative increase of strange particles across different colliding systems and energies, the yield ratios are presented as a function of the mean charged-particle multiplicity density. Figure 6 shows the multiplicity dependence of the yield ratios of p, K_S^0, Λ, ϕ, Ξ and Ω to the pion yield in pp collisions at $\sqrt{s} = 7$ TeV and 13 TeV, p–Pb collisions at $\sqrt{s_{NN}} = 5.02$ and 8.16 TeV, Pb–Pb collisions at $\sqrt{s_{NN}} = 5.02$ TeV and Xe-Xe collisions at $\sqrt{s_{NN}} = 5.44$ TeV. There is a smooth evolution with multiplicity across different systems, from low-multiplicity pp to high-multiplicity central Pb–Pb collisions. Preliminary Xe-Xe results are consistent with Pb–Pb ones and hint at the fact that hadrochemistry is independent of the nucleus species employed for the collision. The

strangeness enhancement is found to be more pronounced for particles with a larger strangeness content. The zero net-strangeness (S = 0) ϕ-meson exhibits an intermediate behavior between K_S^0 (S = 1) and Ξ (S = 2). It is observed that the production of strange particles is collision-energy independent at a given multiplicity.

4. Conclusions

ALICE has measured strangeness production in pp, p–Pb, Xe–Xe and Pb–Pb collisions. In Pb–Pb collisions a hardening of strange hadron transverse momentum spectra is observed, with increasing centrality (radial flow). A similar effect is also present in pp collisions at $\sqrt{s} = 7$ TeV and 13 TeV with increasing multiplicity. Strangeness enhancement is observed in high multiplicity pp collisions. Strange particle-to-pion ratios evolve smoothly with charged-particle multiplicity, regardless of the collision system and energy.

References

[1] Rafelski J and Muller B 1982 *Phys. Rev. Lett.* **48** 1066
[2] Abelev B(ALICE Collaboration) *et al* 2008 *JINST* **3** S08002
[3] Song H and Heinz U W 2008 *Phys. Lett.* B **658** 279
[4] Fries R J *et al* 2008 *Annu. Rev. Nucl. Part. Sci.* **58** 177
[5] Werner K 2012 *Phys. Rev. Lett.* **109** 102301
[6] Adam J *et al* (ALICE Collaboration) 2017 *Nat. Phys.* **13** 535
[7] Sjostrand T, Mrenna S and Skands P Z 2008 *Comput. Phys. Commun.* **178** 852
[8] Pierog T *et al* 2015 *Phys. Rev.* C **92** 034906
[9] Bierlich C and Christiansen J R 2015 *Phys. Rev.* D **92** 094010